Electronic Supplementary Material (ESI) for Dalton Transactions.

Electron Transfer Mechanism of Catalytic Superoxide Dismutation *via* Cu(II/I) Complexes: Evidence of Cupric-superoxo/-hydroperoxo Species

Ram Chandra Maji,[a] Partha Pratim Das,[b] Anirban Bhandari,[a] Saikat Mishra,[a]

Milan Maji[a] and Apurba K. Patra[a]*

[a]Department of Chemistry, National Institute of Technology Durgapur, Mahatma Gandhi Avenue, Durgapur 713 209, India;

[b]Department of Chemistry, Indian Institute of Technology Kanpur, Kanpur 208 016, India.

Table of contents

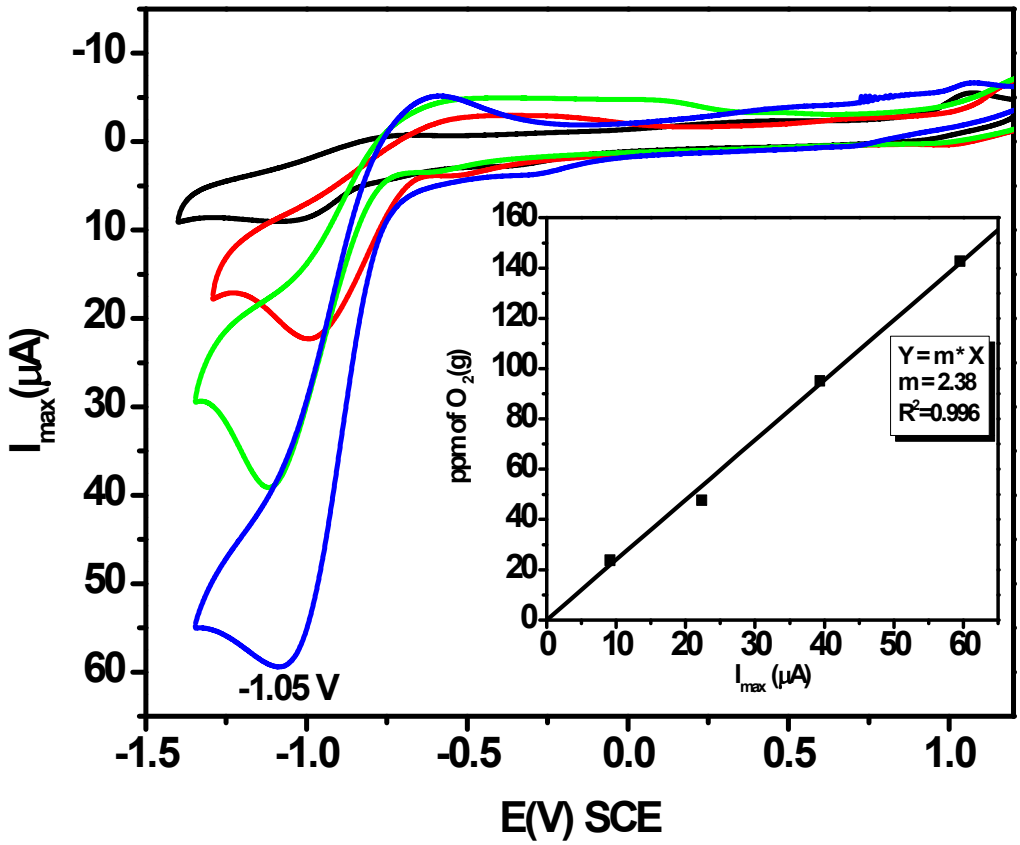

Fig. S1: Cyclic voltammograms of O_2 dissolved in 6 mL CH_3CN solution containing $(Bu_4N)ClO_4$ as supporting electrolyte at 298 K at a platinum working electrode at a scan rate of 100 mV s^{-1} using *SCE* as reference electrode: [O_2] are 0.1 mL (23.83 ppm, black trace), 0.2 mL (47.67 ppm, red trace), 0.4 mL (95.17 ppm, green trace), 0.6 ml (142.83 ppm, blue trace); maximum i_{pc} observed electrochemically are 9.1, 22.32, 39.30 and 59.49 respectively. Inset: Standardization plot.

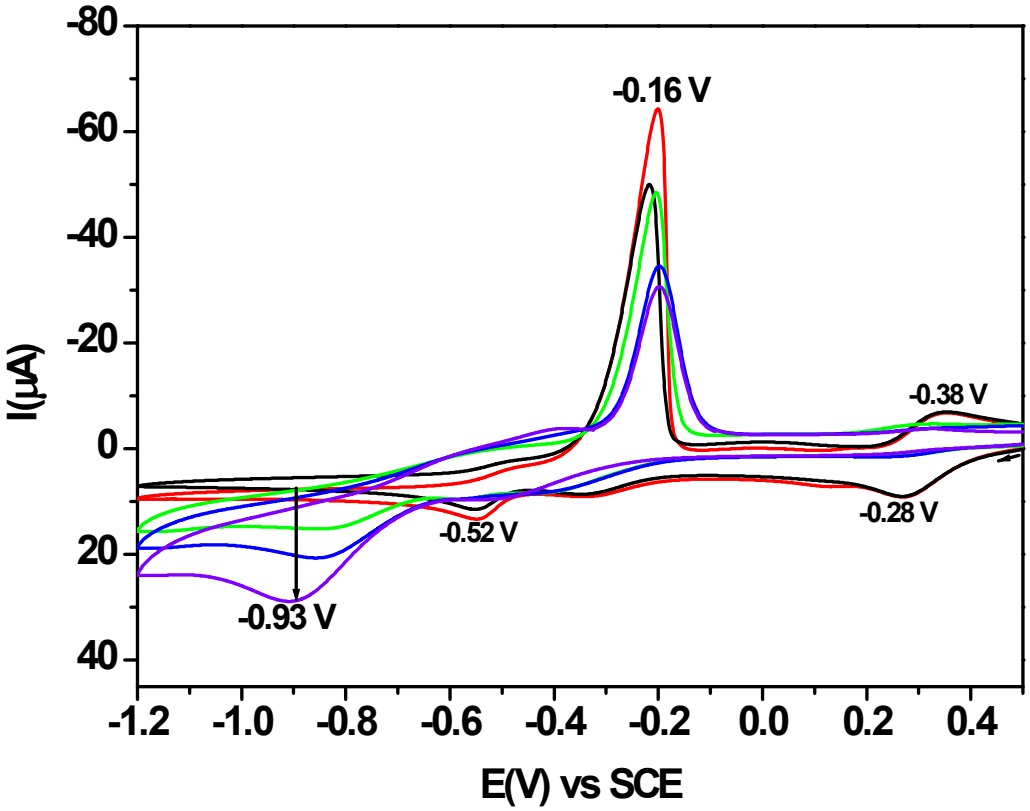

Fig. 4, Top in the main text: Cyclic voltammograms in CH_3CN containing 0.1 M $[(n\text{-}Bu)_4N]ClO_4$ as a supporting electrolyte at 298 K at a platinum working electrode at a scan rate of 100 mV s^{-1} using SCE as reference electrode of **1** in CH_3CN (Black trace), then after adding KO_2 repeated scans until reach to a maximum i_{pc} (green→blue→violate) at -0.93 V. Red trace after purging of N_2 (g) to complete remove of O_2(g) produced. Calculated amount of O_2(g) evolution is 97%.

Calculation for liberated O_2(g) from reaction of 2 in 6 mL CH_3CN with KO_2.

I_{max}(A) obtained at -0.93 V after addition of KO_2 to a CH_3CN solution of 10 mg of **1** (or 13.16 x10^{-3} mmol of **1**) = 28.58 μA (See Fig. S21). From the slope of the calibration plot (See Fig. S20) this I_{max} correspond to 2.38 x 28.58 = **8.02 ppm** of O_2(g) that is liberated from a 13.16 x10^{-3} mmol of **1** in CH_3CN.

F.Wt. of **2** = 759.4

1 + KO_2 = **2** + O_2 (g)

759.4 gm of **1** will liberate 32 gm of O_2 (g) at NTP

Then, 10 mg of **1** will liberate 0.4214 mg of O_2 (g) at NTP

This, 0.4214 mg of O_2(g) is dissolved in 6 ml of CH_3CN = (0.4214 x 1000)/6 = **70.23 ppm** of O_2 (g) [ppm = mg/L]

If **70.23 ppm** O_2 (g) liberates then it will be 100% O_2 (g) evolution, however the liberated amount of O_2(g) is **68.02 ppm**.

Therefore yield % of O_2(g) evolution = (68.02 x 100)/70.23 = 97%

a)

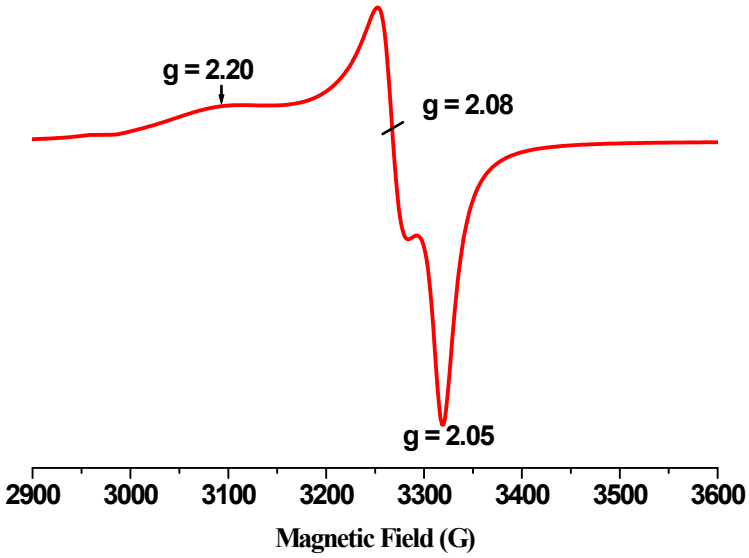

b)

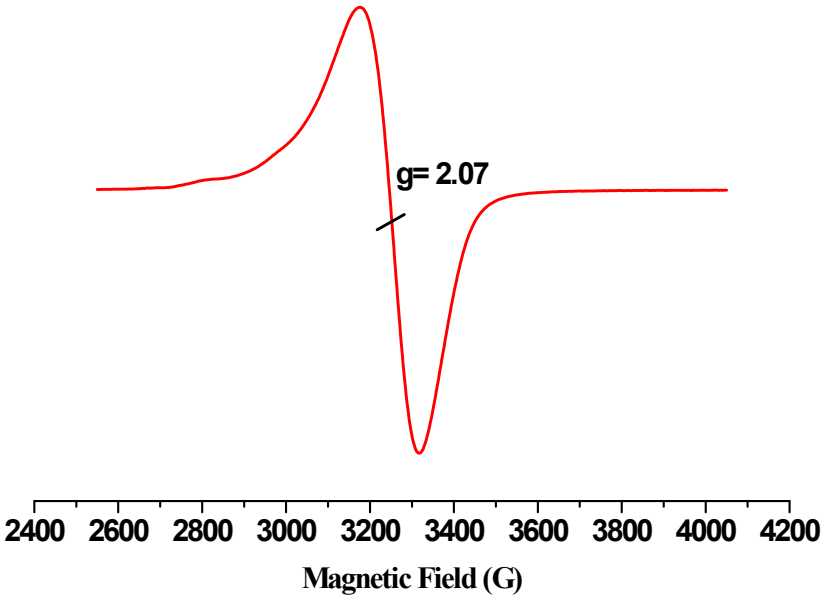

Fig. S2: X-Band EPR spectrum of (a) solid **1** at 77 K, (b) of **1** in CH_3CN-toluene solution at 77 K. Spectrometer settings: frequency = 9.456 GHz, power= 0.189 mW, modulation frequency = 100 kHz; modulation amplitude = 5 G and receiver gain = 1 x 10^3 (for solid) and receiver gain = 1 x 10^4 for solution phase measurement.

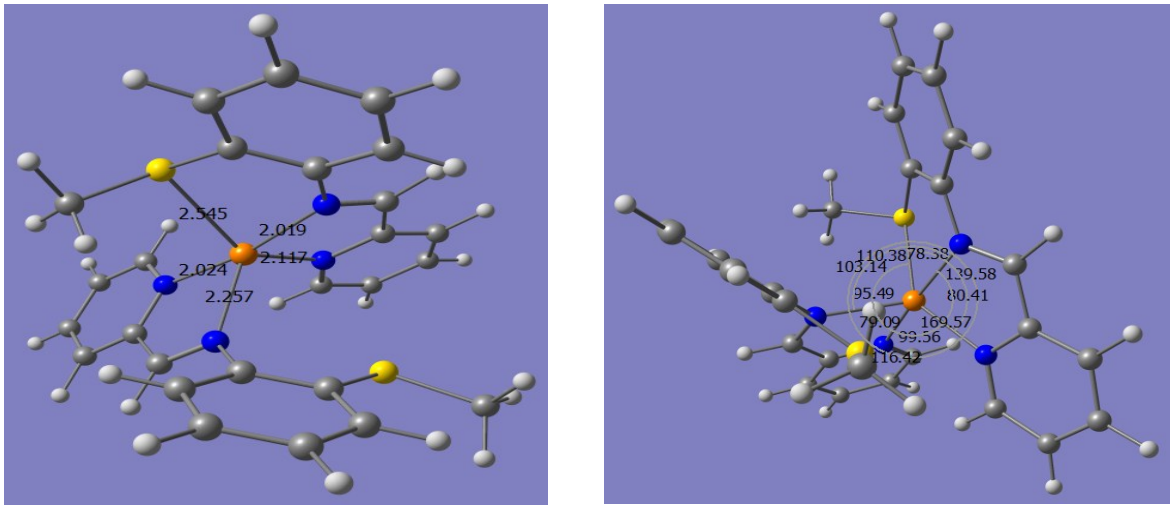

Fig. S3: DFT optimized structures of modelled complex $[(L1)_2Cu]^{2+}$ (Cation of **1**)

Bond distance (Å)	**DFT optimized structure**	**Crystal structure (Fig. 1, top)**
Cu1-N1	2.117	2.017(3)
Cu1-N2	2.024	1.958(3)
Cu1-N3	2.019	1.956(3)
Cu1-N4	2.257	2.153(3)
Cu1-S1	2.545	2.4461(10)
Cu1-S2	3.701	3.667(2)
Bond angle (°)		
N1-Cu1-N2	80.41	81.73(11)
N1-Cu1-N3	103.14	100.72(11)
N1-Cu1-N4	116.42	119.79(11)
N1-Cu1-S1	139.58	142.37(8)
N2-Cu1-N3	169.57	174.82(12)
N2-Cu1-N4	110.38	102.43(11)
N2-Cu1-S1	78.38	80.29(8)
N3-Cu1-N4	79.09	80.39(11)
N3-Cu1-S1	95.49	95.14(8)
N4-Cu1-S1	99.56	96.30(8)

Table S1: Comparison of bond distances and Angles of $[(L1)_2Cu]^{2+}$ optimized structure and X-ray structure of **1**.

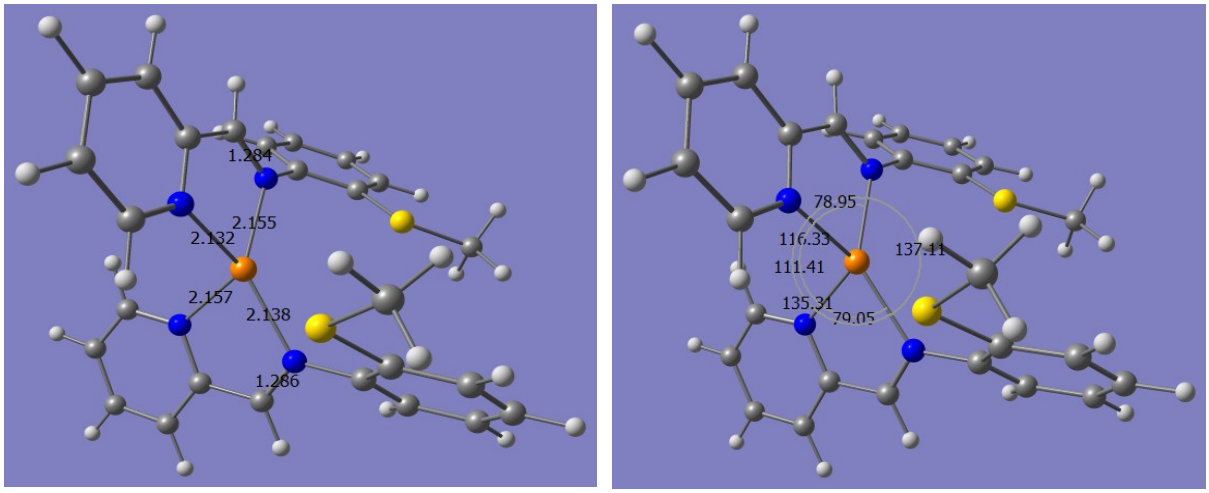

Fig. S4: DFT optimized structures of modelled complex of $[(L1)_2Cu]^+$ (Cation of **2**)

Bond distance (Å)	**Optimized Structure**	**Crystal Structure (Fig.1, bottom)**
Cu1-N1	2.132	2.093(6)
Cu1-N2	2.155	2.019(5)
Cu1-N3	2.138	2.029(5)
Cu1-N4	2.157	2.112(4)
Cu1-S1	3.477	3.212(2)
Cu1-S2	3.357	3.173(2)
Bond angle (º)		
N1-Cu1-N2	79.05	80.7(2)
N1-Cu1-N3	111.41	106.3(2)
N1-Cu1-N4	116.33	112.8(2)
N2-Cu1-N3	137.41	138.7(2)
N2-Cu1-N4	135.31	135.02(19)
N3-Cu1-N4	78.95	80.86(18)

Table S2: Comparison of bond distances and Angles of $[(L1)_2Cu]^+$ optimized structure and X-ray structure of **2**.

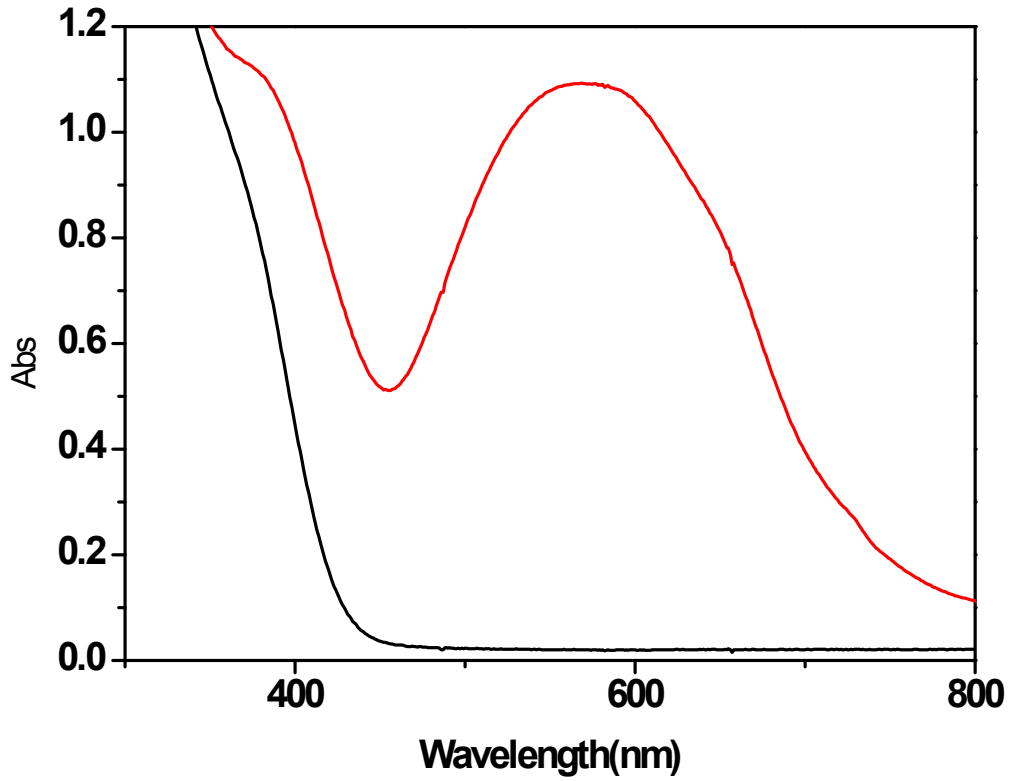

Fig. S5: UV-Vis spectra of 0.030 mM NBT (black trace) and NBT+ DMSO solution of 50 equiv. KO_2 (Red trace) taken in NEM buffer at PH 7.4.

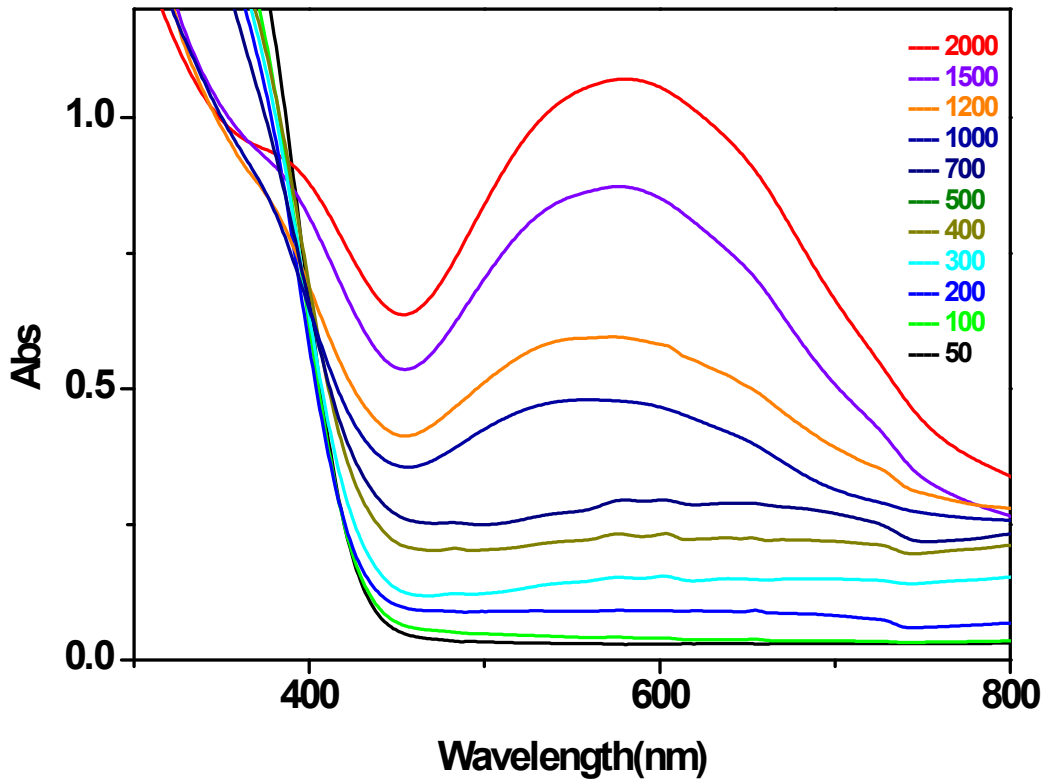

Fig. S6: UV-Vis spectral changes of NBT, treated with various amount of KO_2 in presence of **1** (black→red traces) in NEM buffer at PH 7.4. The numerical values 50 to 2000 are the equivalent amount of KO_2, added to 1 equivalent of complex **1**.

Calculation for % inhibition of NBT assay:

Kinetically the reduction of NBT to formazane has been determined following the absorbance changes at λ= 560 nm using the following equation.

% Inhibition = $\{[(\Delta A_{560nm}/minutes)_{blank}-(\Delta A_{560nm}/minutes)_{sample}]/ (\Delta A_{560nm}/minutes)_{blank}\}X100$

$\Delta A_{560nm}/minutes$ = [A_{560nm} at time 4:30 minutes - A_{560nm} at 0:30 minutes]/4

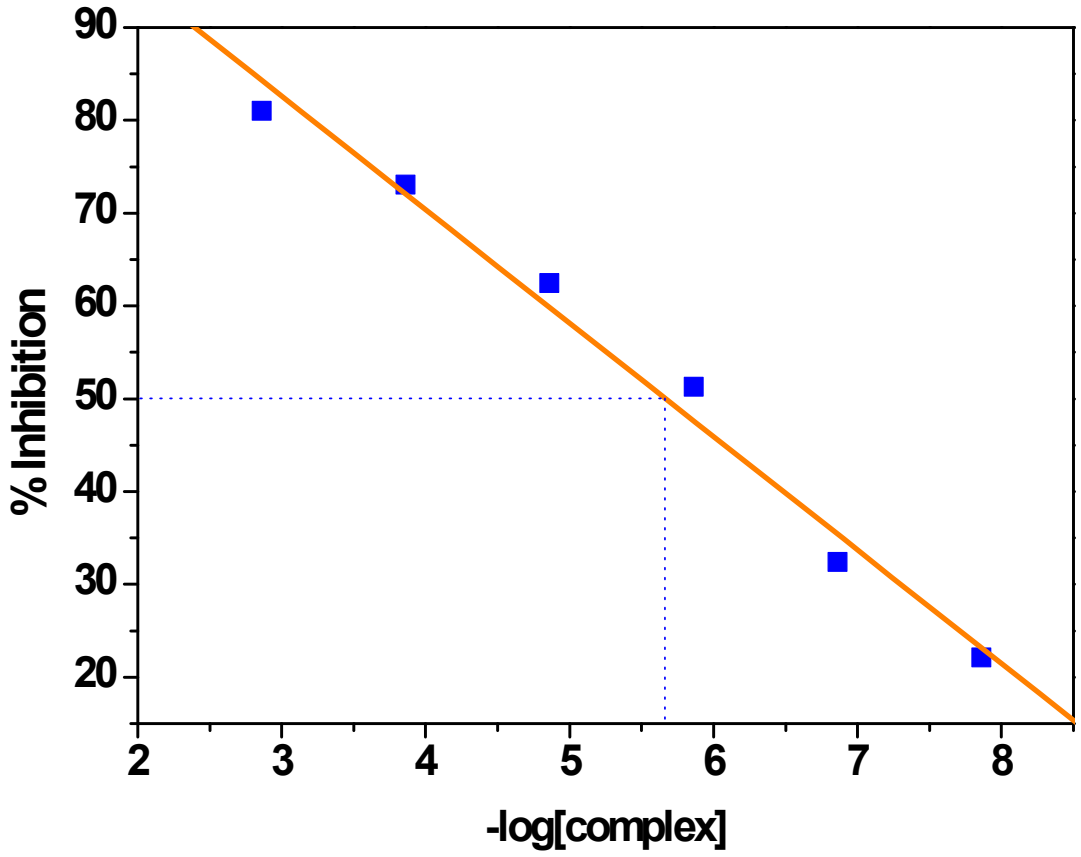

Fig. S7: % inhibition of NBT *vs* –log[complex **1**] plot. The position of 50% inhibition has been shown using dotted lines.

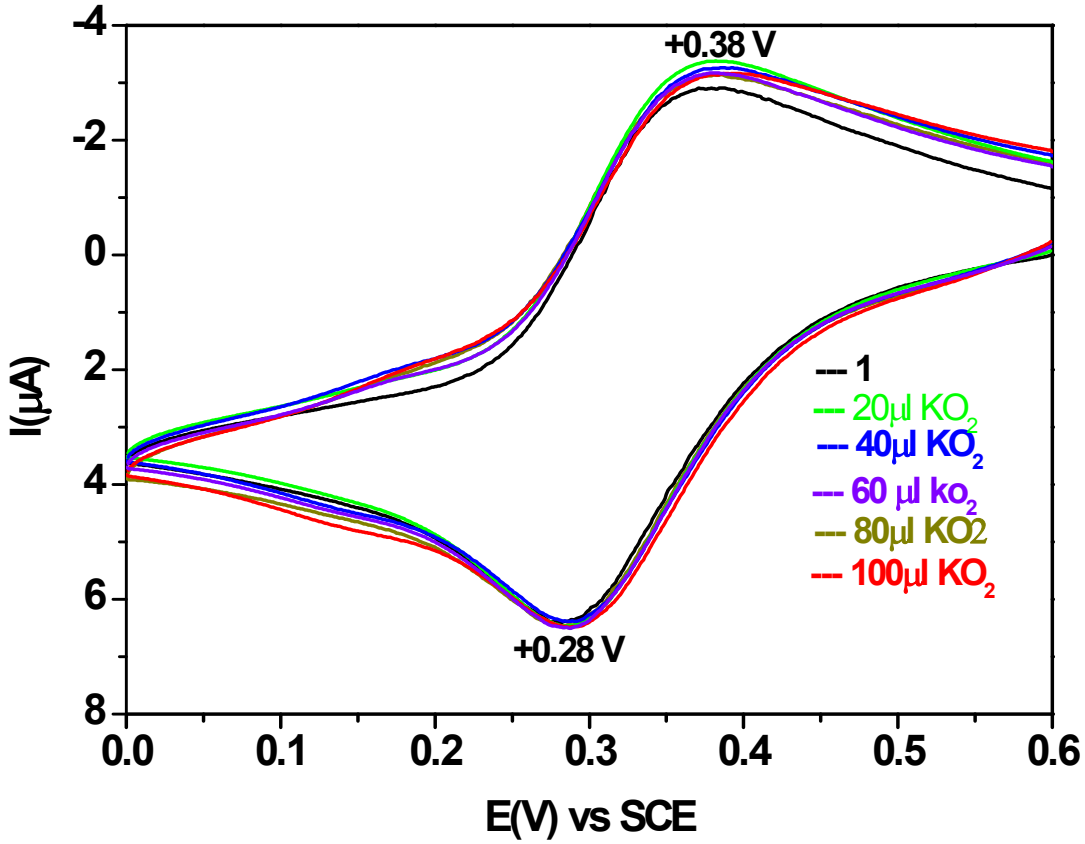

Fig. S8: Cyclic voltammograms of **1** in CH_3CN containing 0.1M $[(n\text{Bu})_4\text{N}]ClO_4$ as a supporting electrolyte at 298K at a Pt working electrode at 50 mV s^{-1} using SCE as reference electrode. Stoichiometric KO_2 was dissolved in 100μl CH_3OH, then 20 μL aliquots were added and after each addition the CV scan was taken.

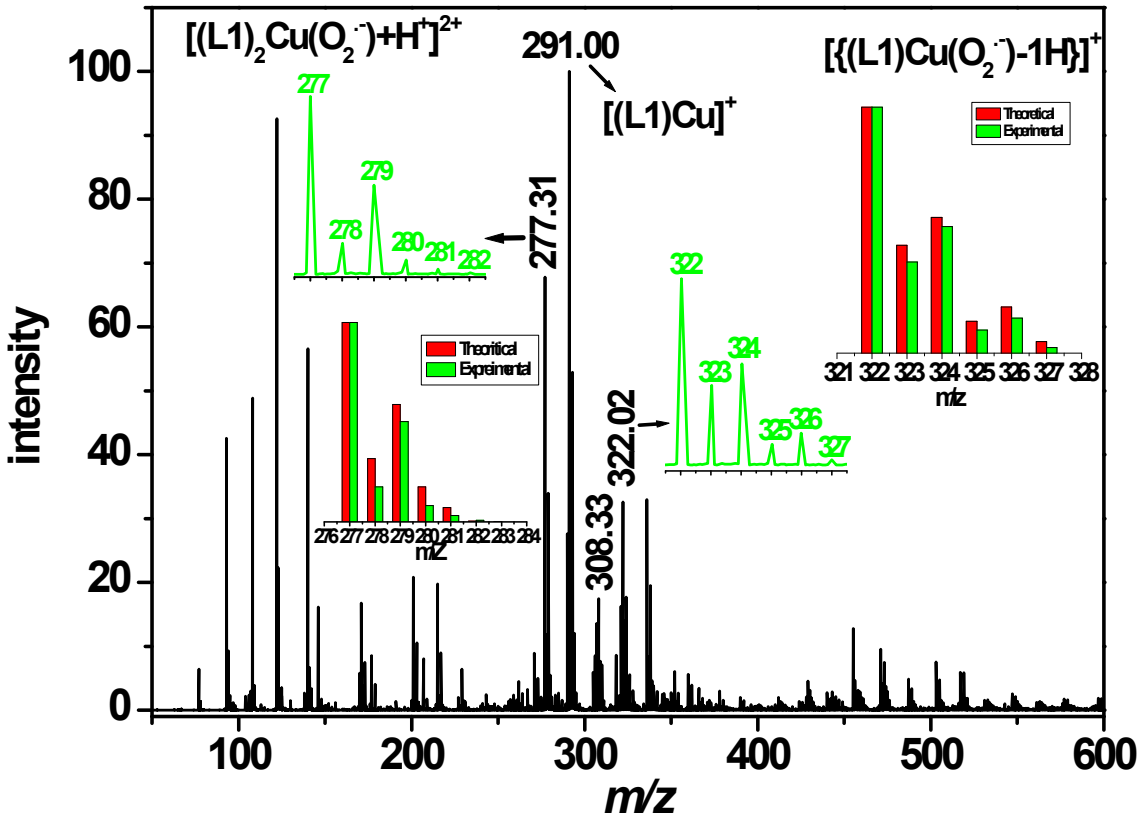

Fig. S9: ESI positive mass spectrum of a solution mixture of **1** + KO_2 made at 233 K in CH_3CN then quickly measured at 298 K. Peak at m/z = 277.31, 291.0037, 308.0098 and 322.02 corresponds to $[(L1)_2Cu(O_2)+1H^+]^{2+}$, $[(L1)Cu]^+$, $[(L1)Cu(O_2)Cu(L)]^{2+}$ and $[\{(L1)Cu(O_2)-1H\}]^+$ respectively. Inset: Isotopic mass distribution, experimental (green) and simulated (red trace) of the corresponding peak marked with arrow.

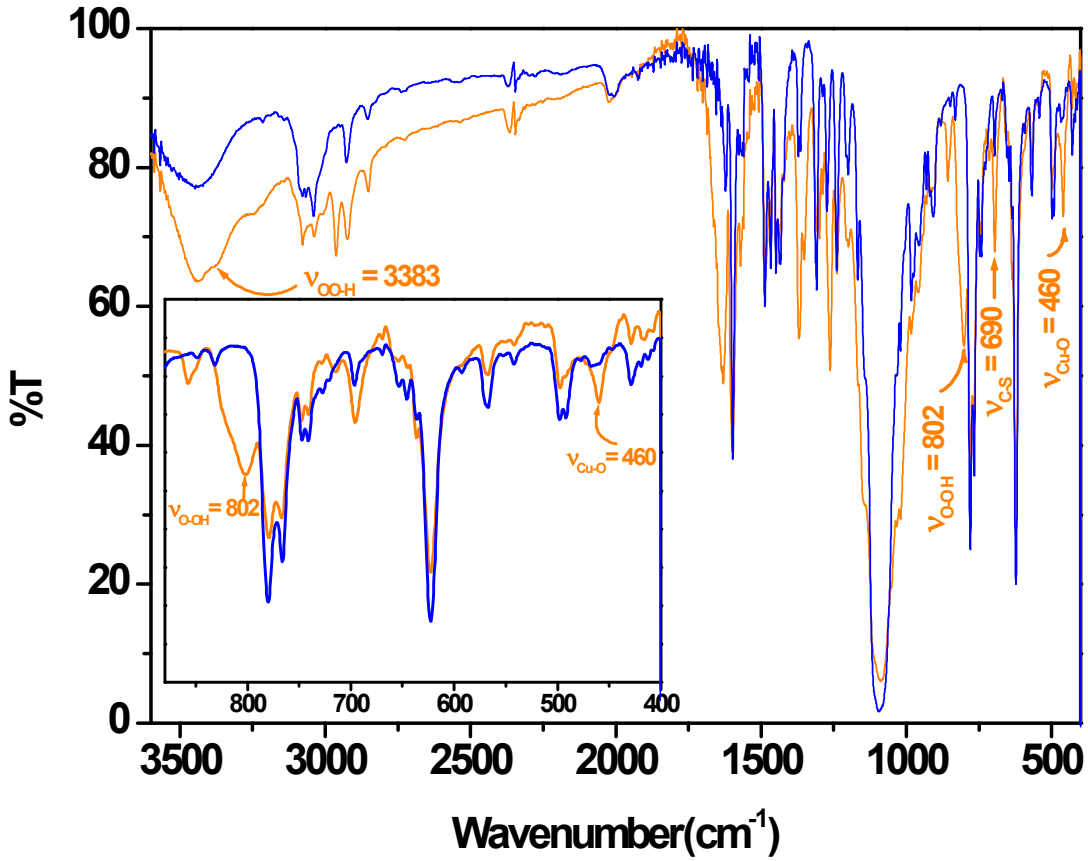

Fig. S10: FTIR spectra of $[(L1)_2Cu](ClO_4)_2.CH_3CN$, **1**.$CH_3CN$, (blue trace) and $[(L1)_2Cu(OOH^-)](ClO_4)$ (orange trace) in KBr disk, shown in the range 400 cm^{-1}-3600 cm^{-1}.

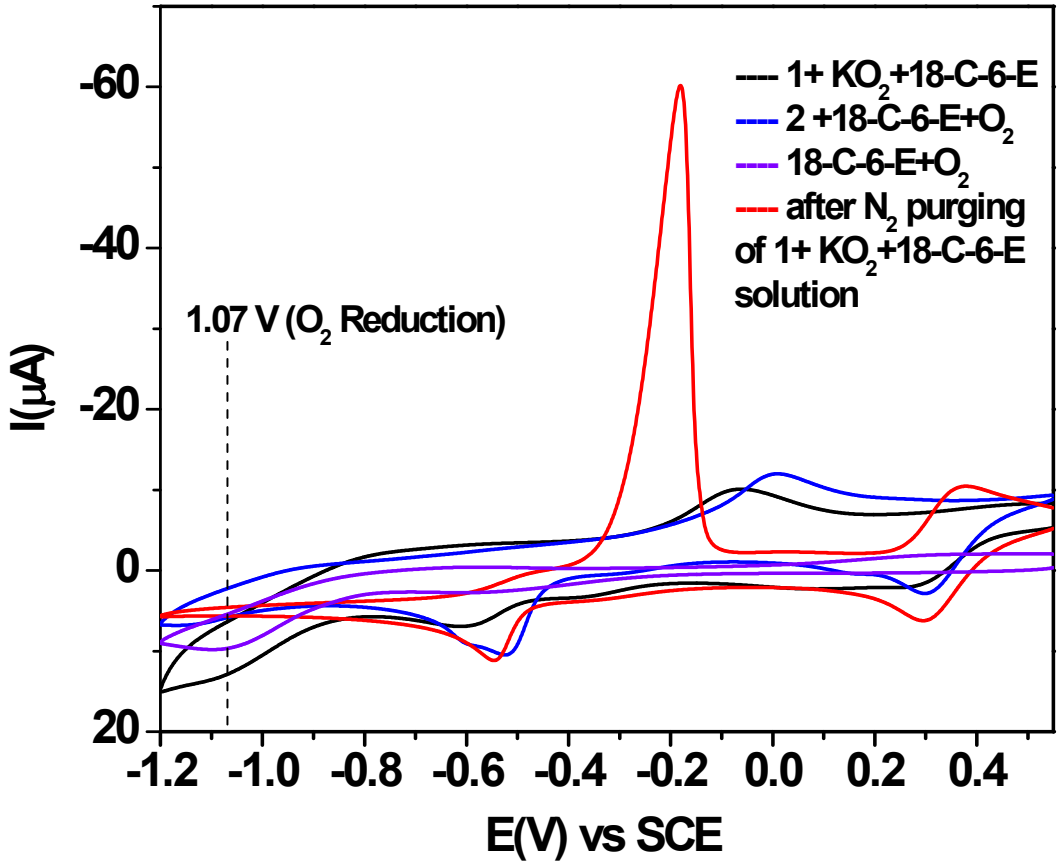

Fig. S11: Cyclic voltammograms in CH_3CN containing 0.1 M $[(n\text{-}Bu)_4N]ClO_4$ as a supporting electrolyte at 233 K at a platinum working electrode at a scan rate of 100 mV s^{-1} using SCE as reference electrode of **1+KO_2+18-C-6-E** in CH_3CN (**Black trace**), **2 +18-C-6-E+O_2** (**blue trace**), **18-C-6-E+O_2** (**violet trace**), after N_2 purging to the mixture of 1+KO_2+18-C-6-E i.e **1+KO_2+18-C-6-E + N_2** (**red trace**).

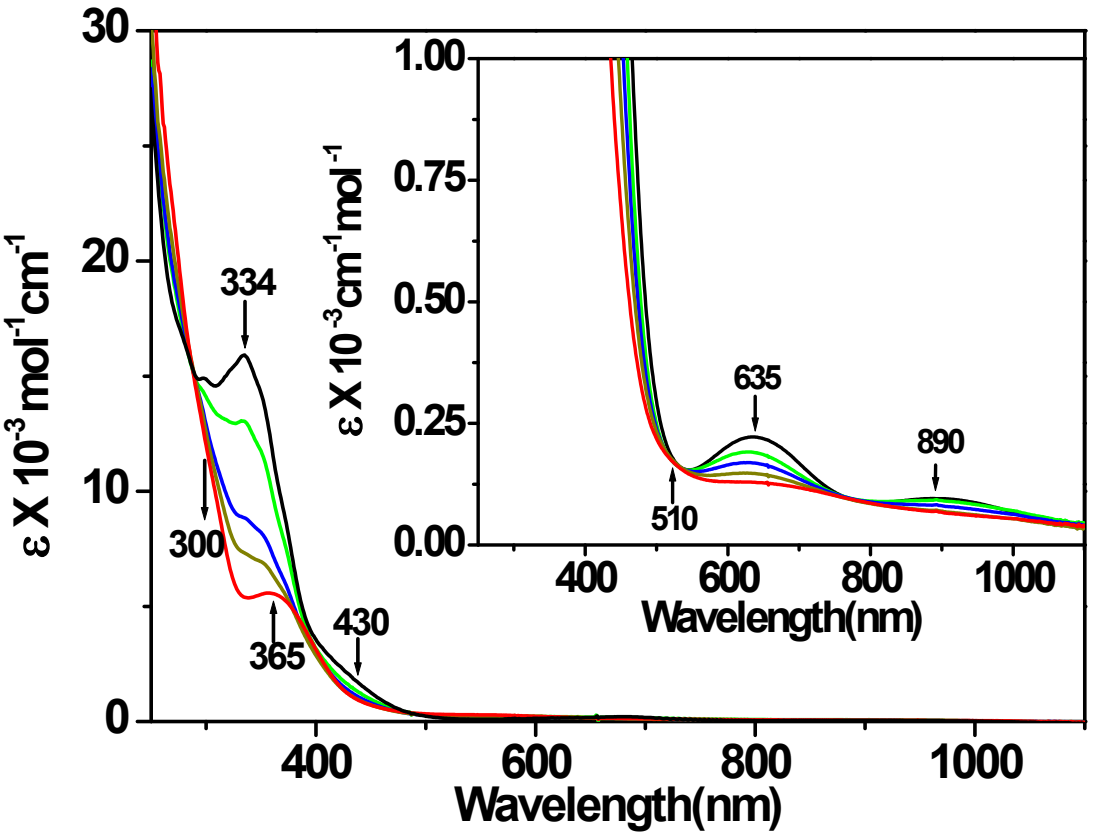

Fig. S12: UV-Vis absorption traces showing conversion of a CH_3CN solution of **1** (1 x 10^{-4} M, black trace) + KO_2 + 18C6E → **2** (red trace) at 233 K, inset: [**1**] = 1 x 10^{-3} M. One equiv. of KO_2 and 18C6E together was dissolved in CH_3CN then added and after each time addition spectrum taken.

a)

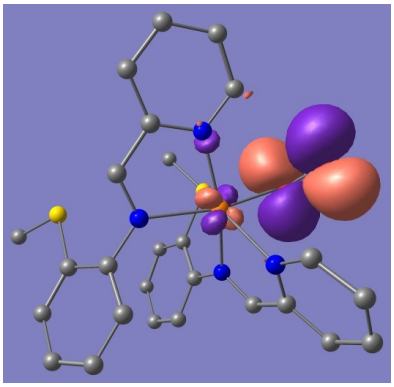

HOMO(α)

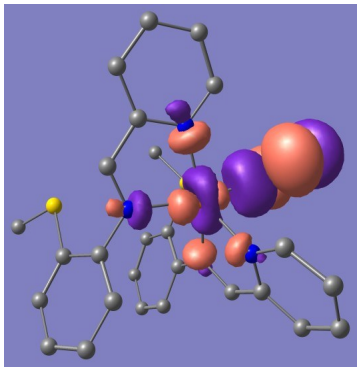

LUMO(α)

	MO number	Energy (ev)	Ligand contribution (%)	Metal contribution (%)	Oxygen contribution (%)
HOMO(α)	137	-0.298404083	8.2	3.6	88.2
LUMO(α)	138	-0.231471565	17.3	25.965	56.73

b)

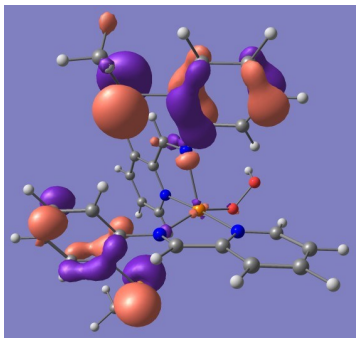

HOMO(α)

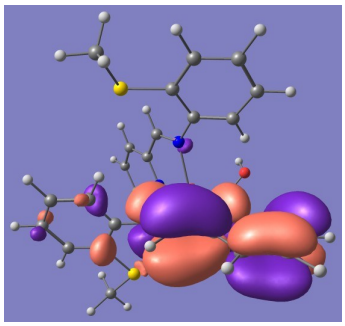

LUMO(α)

	MO number	Energy (ev)	Ligand contribution (%)	Metal contribution (%)	Oxygen contribution (%)
HOMO(α)	138	-0.305387341	96.705	1.675	1.62
LUMO(α)	139	-0.19335202	95.234	4.05	0.716

Fig. S13: Spin density plot of HOMO and LUMO of DFT optimized modelled structure of (a) $[(L1)_2Cu(O_2^{\cdot-})]^+$ and of (b) $[(L1)_2Cu(OOH^-)]^+$. Metal, ligand and oxygen orbital contribution has been shown for each modelled structure in the Tables.

$[(L)_2Cu^{II}O_2^{\cdot -})]^+$	
Bond distances(Å)	
Cu1-N1	2.176
Cu1-N2	2.207
Cu1-N3	2.099
Cu1-N4	2.203
Cu1-O1	2.070
O1-O2	1.261
Bond Angles(^{0})	
N1-Cu1-N2	108.39
N1-Cu1-N3	78.76
N1-Cu1-N4	97.23
N1-Cu1-O1	168.05
N2-Cu1-N3	122.35
N2-Cu1-N4	77.31
N2-Cu1-O1	82.49
N3-Cu1-N4	160.30
N3-Cu1-O1	91.49
N4-Cu1-O1	89.87

Table S3: Bond distances and Bond Angles of DFT optimized structure of $[(L)_2Cu^{II}O_2^{\cdot -})]^+$.

$[(L)_2Cu^{II}$-OOH)$]^+$	
Bond distances(Å)	
Cu1-N1	2.357
Cu1-N2	2.091
Cu1-N3	2.075
Cu1-N4	2.199
Cu1-O1	1.966
O1-O2	1.425
Bond angles(^{0})	
N1-Cu1-N2	105.54
N1-Cu1-N3	76.46
N1-Cu1-N4	92.87
N1-Cu1-O1	108.59
N2-Cu1-N3	175.48
N2-Cu1-N4	77.51
N2-Cu1-O1	92.09
N3-Cu1-N4	98.42
N3-Cu1-O1	91.08
N4-Cu1-O1	158.08

Table S4: Bond distances and Bond Angles of DFT optimized structure of $[(L)_2Cu^{II}O_2H)]^+$.

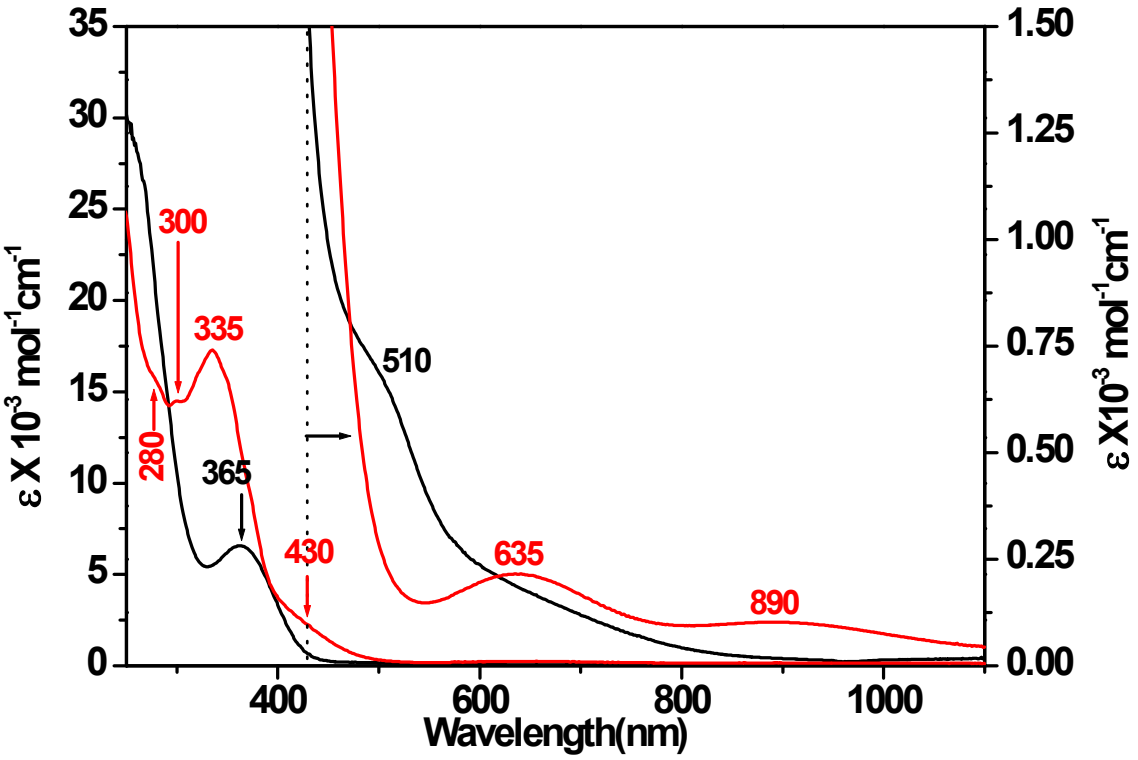

Fig. S14: UV-Vis spectra of $[(L1)_2Cu](ClO_4)_2.CH_3CN$, **1**.$CH_3CN$, (red trace) and $[(L1)_2Cu](ClO_4)$, **2**, (black trace) in CH_3CN.

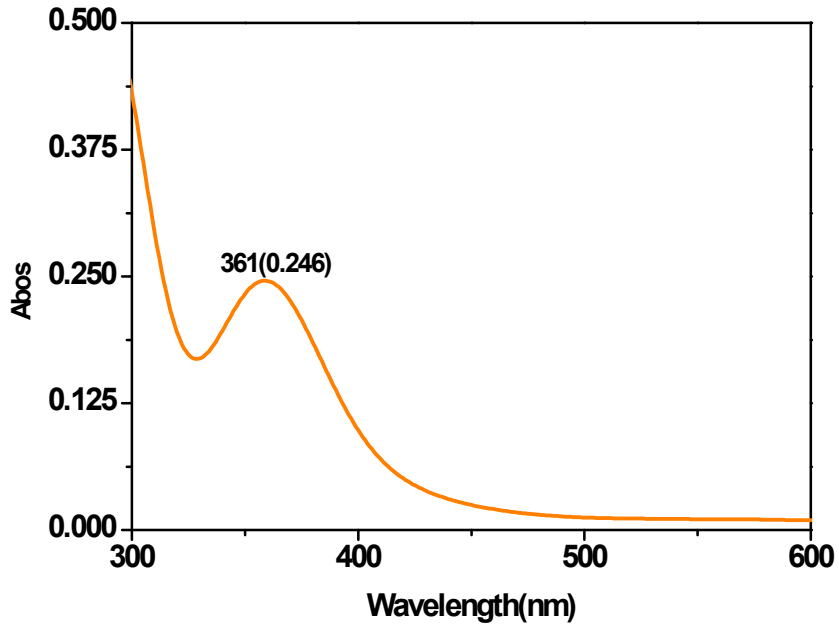

Fig. S15: UV-Vis spectrum of I_3^- generated from the reaction **2**+KO_2+2$HClO_4$ + (excess) NaI → I_3^- . (**2**+ KO_2+ 2$HClO_4$ → **1** + H_2O_2, H_2O_2+$HClO_4$ + I^- → I_2 , I_2+I^- → I_3^-).

Calculation for the amount of H_2O_2 liberated from reaction:

Concentration of **2** =10^{-4} M

$\varepsilon = 2.5 \times 10^4\ M^{-1}\ cm^{-1}$

A=0.246

Hence C= (ε/A) M

= (0.246/2.5 X 10^4) M

= 0.098 X 10^{-4} M

Since the solution was diluted 10 times

Hence concentration of H_2O_2 = (0.098 X 10^{-4}) M X 10

= 0.98 X 10^{-4} M

Hence % of **H_2O_2 =98 %.**

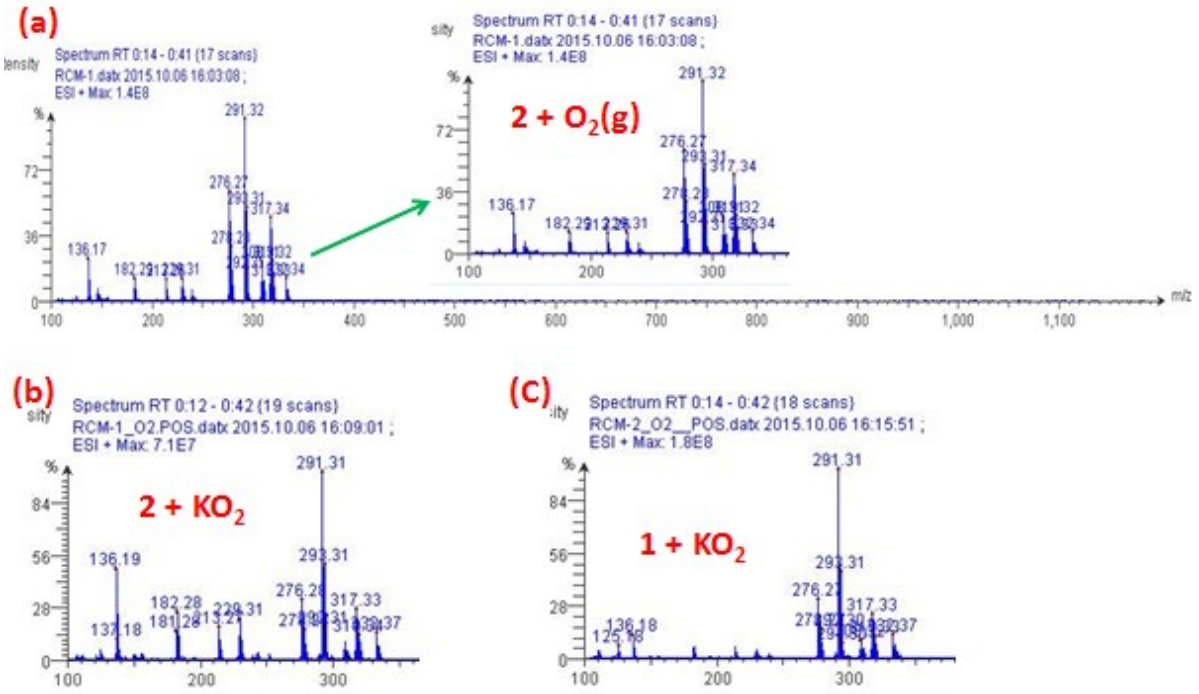

Fig. S16: ESI positive mass spectrum of **1** and **2** in the range 100-1200: CH_3CN solution of **1** and **2** were frozen at 77 K, (a) To frozen solution of **1** + O_2(g), (b) frozen solution of **2** + KO_2, (c) frozen solution of **1** + KO_2 when melt the sample injected for mass spectrum. Spectral profile looks same for all three reactions indicates progress to achieve the final $[(L1)_2Cu(OOH^-)]^+$ product. So we did the higher resolution mass spectra of (b), see **Fig. S9:** for peak assignment.

This experiment support, $[(L1)_2Cu^I]+O_2 \rightarrow \{[(L1)_2Cu(O_2^{\cdot-})]^+ \leftrightarrow [(L1)_2Cu(O_2^{2-})]\} \rightarrow [(L1)_2Cu(OOH^-)]^+$ conversion.